Kobe J. Med. Sci., Vol. 56, No. 4, pp. E154-E161, 2010

Comparison of Capability of Abdominal 320-Detector Row CT and of 16-Detector Row CT for Small Vasculature Assessment

RYO SUGIHARA[1], KAZUHIRO KITAJIMA[1], TETSUO MAEDA[1,2], TAKESHI YOSHIKAWA[1*], MINORU KONISHI[2], NAOKI KANATA[1], TOMONORI KANDA[1], HISANOBU KOYAMA[1], DAISUKE TAKENAKA[1], YOSHIHARU OHNO[1,2], and KAZURO SUGIMURA[1]

[1]*Department of Radiology, Kobe University Graduate School of Medicine, Kobe, Japan*

[2]*Division of Radiology, Kobe University Hospital, Kobe, Japan*

Received 14 June 2010/ Accepted 7 July 2010

Key Words: 320-detector row CT, abdomen, vasculature

The purpose of our study was to compare the capability of the 320-detector row CT (area-detector CT: ADCT) using the step-and-shoot scan protocol for small abdominal vasculature assessment with that of the 16-detector row CT using the helical scan protocol. Contrast-enhanced abdominal CT for preoperative assessment was administered to 25 patients, 18 of whom, suspected of having lung cancer, underwent ADCT using the step-and-shoot scan protocol, while the remaining 7, suspected of having renal cell carcinoma, underwent 16-MDCT using the helical scan protocol. Two experienced abdominal radiologists independently assessed renal interlobar and arcuate as well as mesenteric marginal (Griffith point) arteries by means of a 5-point visual scoring systems. Kappa analysis was used for evaluation of interobserver agreement. To compare the visualization capability of the two systems, the scores for each of the arteries were compared by using the Mann-Whitney U-test. Overall interobserver agreements for both systems were almost perfect ($\kappa>0.78$). Visualization scores for renal interlobar and arcuate, ($p<0.0001$) and mesenteric marginal (Griffith point) arteries ($p<0.05$) were significantly higher for ADCT than for 16-detector row CT. ADCT using the step-and-shoot scan protocol for small abdominal vasculature assessment can be considered superior to 16-detector row CT using the helical scan protocol.

INTRODUCTION

Accurate preoperative assessment of abdominal small vessels is an essential step for effective and efficient abdominal surgical and radiological interventions. Contrast-enhanced dynamic computed tomography (CT) with three-dimensional and multiplanar (MPR) image reconstruction has been used for this purpose. Developments in CT technology, especially optimized detector geometry with thinner slice collimation and increased gantry rotation speed, have improved temporal and spiral resolution as well as visualization of small abdominal vessels and detection of anomalies [1-6].

A new generation of CT systems with 320-detector rows (Area-detector CT or ADCT) has recently become clinically available, making volumetric imaging possible. The ADCT

Phone: +81-78-32-6104 Fax: +81-78-382-6129 E-mail: yoshikaw@med.kobe-u.ac.jp

system offers a single rotational acquisition, which covers 16 cm in the z-direction and avoids interslice stitching artifacts and data interpolations, which is a substantial improvement over standard helical CT acquisitions using single- and multi-detector row CT systems. With this system, a complete volume data set covering the entire heart and/or brain can be acquired at a single rotation, and several investigators have discussed the utility of ADCT for cardiac and brain imaging [7-11].

However, when the ADCT system is used for abdominal imaging, acquisition of whole abdominal CT images currently requires the use of a conventional helical scan protocol or a step-and-shoot scan protocol with 320-detector rows. In addition, no reported studies have dealt with whole abdominal imaging using ADCT. We hypothesized that ADCT using the step-and-shoot protocol would have the same or better potential compared with that of 16-detector row CT for small abdominal vasculature assessment.

The purpose of this study was therefore to determine the validity of this hypothesis by comparing the capability for small abdominal vasculature assessment of a 320-detector row CT using the step-and-shoot scan protocol with that of a 16-detector row CT using the helical scan protocol.

MATERIALS AND METHODS

Patient population

Prospective contrast-enhanced abdominal CT for preoperative assessment using an ADCT or 16-MDCT system was administered to 25 patients, 18 of whom (13 males, 5 females; mean age: 71.2 yrs) were suspected of having lung cancer and were examined with an ADCT (Aquilion ONE; Toshiba Medical Systems, Otawara, Japan) using the step-and-shoot scan protocol (ADCT group) between July 2008 and March 2009. The remaining 7 patients (6 males, 1 female; mean age: 58.9 yrs) were suspected of having renal cell carcinoma and were examined with a 16-MDCT (Brilliance CT 16, Phillips Healthcare, Best, the Netherlands) using the helical scan protocol (16-MDCT group) between December 2006 and July 2008. Body weight and body mass index (BMI) were obtained from the patient chart. Risk of arterial damage (including history of myocardial infarction, angina pectoris, hypertension, diabetes mellitus, arteriosclerosis obliterans, or dialysis on the charts) was recorded.

This study was approved by the local ethics committee of our institution and informed consent was obtained from all participating patients.

Data acquisition and processing

ADCT examinations were performed with the following parameters: 200-320×0.5 mm detector collimation, 0.35 sec/ gantry rotation, 120 kVp, 400 mA, and 3-5 rotations. Each subject was first examined with unenhanced CT. Next, 80 ml of iodinated contrast medium (Iopamiron 370; Bayer Schering Pharma, Osaka, Japan) was injected at a rate of 3.0 ml/sec followed by 20 ml of saline solution at the same rate, and this was followed by tri-phasic contrast-enhanced CT scans with delay times of 40, 70, and 150 seconds after the start of injection. All four scans covered the area from the diaphragm to the pelvic floor.

For the 16-detector row CT group, examinations were performed with the following parameters: 16×0.75 mm detector collimation, 0.75 sec/gantry rotation, 120 kVp, 250 mA, and 0.813 beam pitch. Each subject was first examined with unenhanced CT. This was followed by the injection of 90 ml of iodinated contrast medium (Iopamiron 370; Bayer Schering Pharma) at a rate of 3.0 ml/sec and then of 20 ml of saline solution at same rate. The scanning protocol for 16-detector row CT consisted of unenhanced and tri-phasic

contrast-enhanced CT scans during the arterial, corticomedullary, and nephrographic phases. Scan delays were 25-30 seconds for the arterial phase using automatic triggering, 60 seconds for the corticomedullary phase, and 120 seconds for the nephrographic phase. For both the unenhanced CT and nephrographic phase CT images, the scan range was set from the diaphragm to the biacetabular line and for arterial and corticomedullary phase images, from the diaphragm to bifurcation of the aorta.

Image Analysis

Two experienced abdominal radiologists, one with 8 and the other with 14 years experience, independently assessed the visualization on a picture archiving and communication system (PACS) workstation (ShadeQuest; Yokogawa Electric Corporation, Musashino, Japan) of renal interlobar and arcuate as well as mesenteric marginal (Griffith point) arteries on arterial-dominant phase axial and coronal reconstructed images. These arteries were selected for the assessment because of their clinical importance [12-15] as well as their locations which can cause image degradation due to motion or intestinal gas, or reduced arterial contrast due to parenchymal enhancement.

For the assessment, a 5-point visual the following scoring system was used: 5, more than two-thirds of the artery was clearly traceable; 4, more than one-third was clearly traceable; 3, less than one-third was traceable; 2, presence of the artery was doubtful due to overall indistinct demarcation; and 1, the artery was entirely untraceable. The length of a mesenteric marginal artery was defined as the distance between the end of the ascending branch of the left colic artery and the end of the left middle colic artery (Griffith point). Renal interlobar and arcuate arteries assessed by ADCT were located in the upper, middle, and lower parts of the bilateral kidneys (a total of 108 parts for 18 patients). Renal interlobar and arcuate arteries assessed by 16-MDCT on the other hand were located in the upper, middle, and lower parts of an unaffected kidney (a total of 21 parts for 7 patients). The arterial-dominant phase was determined as the time when contrast-enhanced CT images obtained, that is, 40 seconds after the injection of the contrast medium for ADCT and 25-30 seconds after the injection of the contrast medium for 16-MDCT.

Statistical analysis

The unpaired t-test was used for comparison of patient characteristics for the two groups, as well as age, body weight, and BMI. To determine the interobserver agreement for small vasculature assessment in the abdomen, the kappa statistics were evaluated as: poor agreement ($\kappa < 0.01$); low agreement ($\kappa = 0.01–0.20$); moderate agreement ($\kappa = 0.21–0.40$); good agreement ($\kappa = 0.41–0.60$); substantial agreement ($\kappa = 0.61–0.80$); and almost perfect agreement ($\kappa = 0.81–1.00$) [16]. For comparison of visualization capability of the ADCT and 16-detector row CT systems, the visually assessed scores for every vessel examined with the two methods were compared by using the Mann-Whitney U-test.

A p value of less than 0.05 was considered statistically significant.

RESULTS

All ADCT and 16-detector row CT examinations were successfully performed, and no adverse effects were observed in this study. Representative cases are shown in Figures 1 and 2.

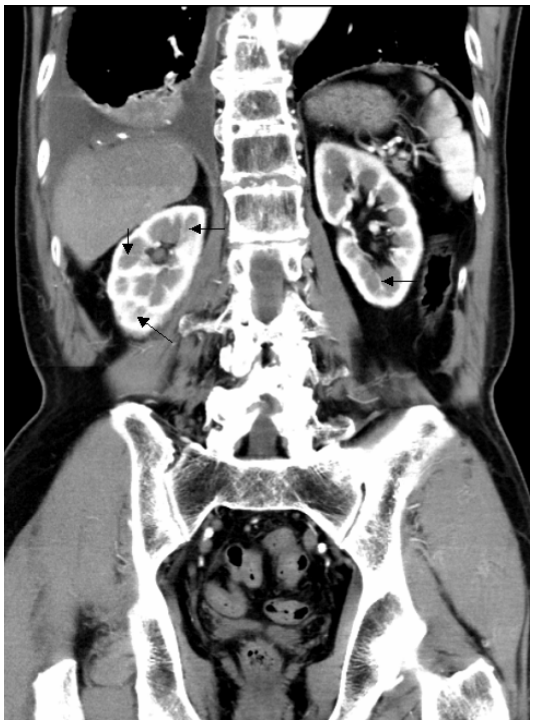

Figure 1. 77-year-old female in ADCT group. Coronal reconstructed 320-detector row CT images using step-and-shoot scan protocol clearly shows bilateral renal interlobar and arcuate arteries (arrows). Visualization was assigned a score of 5.

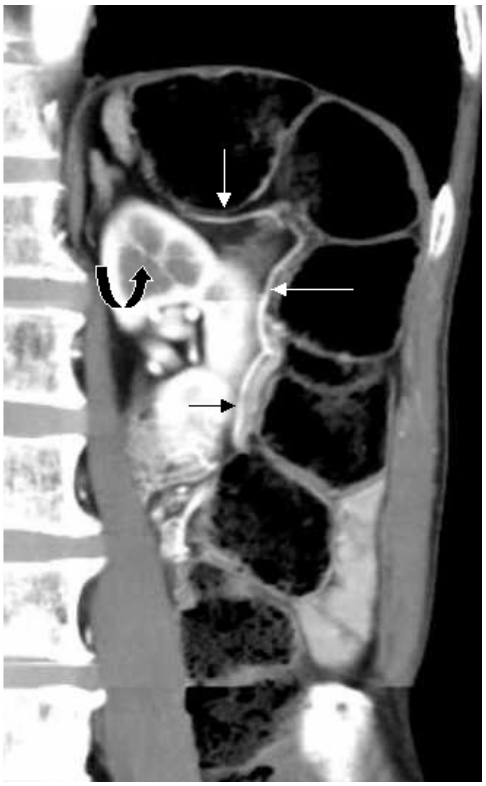

Figure 2. 64-year-old male in ADCT group. Coronal reconstructed 320-detector row CT image using step-and-shoot scan protocol clearly shows mesenteric marginal artery (Griffith point) (arrows) and left renal interlobar and arcuate arteries (curved arrow). Visualization of both arteries was assigned a score of 5.

Comparisons of age, body weight, and BMI for the ADCT and 16-detector row CT groups as seen in Table I show no significant differences between the two groups for any of the parameters ($p>0.05$). As for risks of arterial damage, 5 patients in ADCT group and 2 in 16-MDCT group had hypertension, 1 patient in ADCT group had diabetes mellitus, and no patient had history of myocardial infarction, angina pectoris, arteriosclerosis, or dialysis obliterans, showing no significant differences between the groups.

Figure 3. 47-year-old male in 16-MDCT group.
Coronal reconstructed 16-detector row CT image using helical scan protocol clearly shows left renal interlobar and arcuate arteries (arrows). However, less than one-third of mesenteric marginal artery (Griffith point) was traceable (arrowhead). Visualization of the arteries was assigned a score of 5 and 3, respectively.

Table I. Comparison of Age, Body Weight, and BMI for the Two Groups

	ADCT group (n = 18)	16-MDCT group (n = 7)	p value
Age*	71.2 ± 11.1 (46-82)	58.9 ± 13.3 (44-74)	0.056
Body weight (kg)*	56.5 ± 12.9 (35-83)	65.9 ± 9.8 (54-79)	0.072
BMI (kg/m^2)*	21.7 ± 4.2 (13.5-29.4)	23.5 ± 2.5 (19.6-26.1)	0.21

*Values indicate mean ± standard deviation (range).
ADCT: Area-detector CT (320-detector row CT); BMI: Body mass index

Visualization scores and kappa values are shown in Table II. Interobserver agreement for every artery in both groups was assessed as substantial or almost perfect ($\kappa > 0.78$). In addition, overall kappa values for the ADCT and 16-MDCT groups were 0.86 and 0.87 respectively, thus almost perfect. The consensus values for the two observers were therefore used for further analysis of visual assessment.

Table II. Kappa Values for Vessels of the Two Groups

Artery	ADCT group (n = 18)	16-MDCT group (n = 7)
Mesenteric marginal	1.0 (n=18)	1.0 (n=7)
Renal interlobar & arcuate	0.78 (n=108)	0.81 (n=21)
Overall	0.86	0.87

ADCT: Area-detector CT (320-detector row CT)

Table III. Visualization Scores for Vessels of the Two Groups

Artery	ADCT group (n=18)	16-MDCTgroup(n=7)	p value
Mesenteric marginal*	4.52 ± 0.69 (n=18)	3.86 ± 0.64 (n=7)	0.044
Renal interlobar & arcuate*	4.98 ± 0.14(n=108)	4.43 ± 0.51 (n=21)	<0.0001

*Values indicate mean ± standard deviation.
ADCT: Area-detector CT (320-detector row CT)

DISCUSSION

Preoperative assessment of abdominal vessels is of vital importance for effective and efficient planning and performance of abdominal surgical and radiological interventions. Noninvasive assessment methods such as contrast-enhanced CT have gained acceptance over the last few decades since conventional catheter-based angiography is relatively expensive, time-consuming and above all, associated with certain risks to the patient including various complications due to arterial catheterization. Several studies have demonstrated that non-invasive multi-detector row CT examinations in combination with angiographic and MPR images provide excellent preoperative anatomic information and can be used instead of conventional catheter-based angiography of the abdomen [1-6].

ADCT has recently been utilized in routine clinical practice, making volumetric imaging possible and providing a maximum of 16-cm acquisition in the z-direction in a single rotation. With a detector width of 16cm, images of nearly the entire upper abdominal organs such as liver, pancreas, and spleen can be acquired in a single rotation, while images of the whole abdomen can be acquired in several scanning steps with reduced scanning time.

Turkvatan et al. reported that the sensitivity and specificity of 16-MDCT for the detection of anatomic variants of renal arteries including accessory arteries and early arterial branching of 59 living renal donors were 100% [1]. Our results constitute the first to demonstrate that ADCT is better for small vasculature assessment than 16-MDCT without any reduction in interobserver agreement.

The implementation of ADCT in routine clinical practice has led to the suggestion that the wider cone-beam angle and scattering radiation may result in misaligned geometry on the ADCT images. In fact, as the number of slices is increased, the divergence of the x-ray beams also increases, which leads to more cone-beam artifacts. However, this misaligned geometry may be reduced and improved by using several image reconstruction algorithms [17-20]. Although image degradation may be due, as suggested, to misaligned geometry and cone-beam artifacts, our results also demonstrated that ADCT using the step-and-shoot scan protocol provides excellent abdominal vascular images that are superior to those obtained with the 16-detector row CT system, and can be used for preoperative small abdominal vasculature assessment in routine clinical practice.

In the field of oncology, moreover, perfusion CT has the potential to play a crucial role in diagnosis, staging, prognostic evaluation, and assessment of biomarkers for monitoring the response to therapies. However, perfusion measurement of abdominal organs and lesions suffers from a limited range for cranio-caudal scans. However, Kobayashi et al. reported that whole liver perfusion imaging was possible by using 256-detector row CT [21]. Greater anatomic coverage would permit comprehensive evaluations of organ function and tumor hemodynamics. Furthermore, ADCT features greater cranio-caudal coverage and can open the door for routine clinical use of volumetric cine and perfusion imaging in the abdominal field.

There are several limitations to this study. First, protocols for the two groups were not the same, and the differences in contrast-enhancement techniques may have affected our results.

Second, the number of patients involved was rather small, so that further studies with larger populations are needed to verify our results. Third, ADCT was used for the lung cancer patients in this study and 16-MDCT for the renal cell carcinoma patients. This might lead to a selection bias and affect our results, since the ADCT group of lung cancer patients may have had cardiovascular diseases such as cardiac dysfunction or vessel stenoses more frequently than the 16-MDCT group, which would have resulted in lower contrast enhancement in the vessels, even though no significant difference was found in risks of arterial damage between the two groups. Finally, we only evaluated a limited number of abdominal arteries and did not assess portal and abdominal veins.

In conclusion, ADCT using the step-and-shoot scan protocol can provide excellent vascular images and can be used for pre-operative small abdominal vasculature assessment in routine clinical practice.

ACKNOWLEDGMENTS

The authors wish to thank Yoshikazu Kotani, M.D., Yoshihiro Nishimura, M.D., Ph.D. (Division of Respiratory Medicine, Department of Internal Medicine, Kobe University Graduate School of Medicine), Yoshimasa Maniwa, M.D., Ph.D., Wataru Nishio, M.D. (Division of Thoracic Surgery, Department of Surgery, Kobe University Graduate School of Medicine), and Masato Fujisawa, M.D., Ph.D. (Department of Urology, Kobe University Graduate School of Medicine) for their contribution to this work.

The authors also wish to express special thanks to Hiroyasu Inokawa, M.S., Nao Kishitani, B.S., Yasuko Fujisawa, B.S. and Naoki Sugihara, M.Eng. (Toshiba Medical Systems) for their outstanding technical assistance.

This work was supported by Toshiba Medical Systems and Bayer Pharma.

REFERENCES

1. **Turkvatan, A., Akinci, S., Yildiz, S., Olcer, T., and Cumhur, T.** 2009. Multidector computed tomography for preoperative evaluation of vascular anatomy in living renal donors. Surg Radiol Anat; **31:**227-235.
2. **Miyoshi, T., Kanematsu, M., Kondo, H., Goshima, S., Tsuge, Y., Hatcho, A., Shiratori, Y., Onozuka, M., Moriyama, N., and Bae, K.T.** 2008. Abdomen: Angiography with 16-detector CT-Comparison of image quality and radiation dose between studies with 0.625-mm and those with 1.25-mm collimation. Radiology; **249:**142-150.
3. **Ferrari, R, De Cecco, C.N., Iafrate, F., Paolantonio, P., Rengo, M., and Laghi, A.** 2007. Anatomical variations of the celiac trunk and the mesenteric arteries evaluated with 64-row CT angiography. Radiol Med; **112:**988-998.
4. **Brennan, D.D., Zamboni, G.A., Raptopoulos, V.D., and Kruskal, J.B.** 2007. Comprehensive preoperative assessment of pancreatic adenocarcinoma with 64-section volume CT. Radiographics; **27:**1653-1666.
5. **Sugita, R., Yamazaki, T., Fujita, N., Naitoh, T., Kobari, M., and Takahashi, S.** 2008. Cystic artery and cystic duct assessment with 64-detector row CT before laparoscopic cholecystectomy. Radiology; **248:**124-131.
6. **De Cecco, C.N., Ferrari, R., Rengo, M., Paolantonio, P., Vecchietti, F., and Laghi, A.** 2009. Anatomic variations of the hepatic arteries in 250 patients studied with 64-row CT angiography. Eur Radiol; **19:**2765-2770.
7. **Steigner, M.L., Otero, H.J., Cai, T., Mitsouras, D., Nallamshetty, L., Whitmore, A.G., Ersoy, H., Levit, N.A., Di. Carli, M.F., and Rybicki, F.J.** 2009. Narrowing the

phase window width in prospectively ECG-gated single hart baet 320-detector row coronary CT angiography. Int J Cardiovasc Imaging**; 25:**85-90.

8. **Rybicki, F.J., Otero, H.J., Steigner, M.L., Vorobiof, G., Nallamshetty, L., Mitsouras, D., Ersoy, H., Mather, R.T., Judy, P.F., Cai, T., Coyner, K., Schultz, K., Whitmore, A.G., and Di Carli, MF.** 2008. Initial evaluation of coronary images from 320-detector row computed tomography. Int J Cardiovasc Imaging; **24:**535-546.
9. **San Millán Ruíz, D, Murphy, K., and Gailloud, P.** 320-multidetector row whole-head dynamic subtracted CT angiography and whole-brain CT perfusion before and after carotid artery stenting: technical note. Eur J Radiol; doi: 10.1016/j.ejrad.2009.03.015
10. **Siebert, E., Bohner, G., Dewey, M., Masuhr, F., Hoffmann, K.T., Mews, J., Engelken, F., Bauknecht, H.C., Diekmann, S, and Klingebiel, R.** 2009. 320-slice CT neuroimaging: initial clinical experience and image quality evaluation. Br J Radiol; **82:**561-570.
11. **Salomon, E.J., Barfett, J, Willems, P.W.A., Geibprasert, S., Bacigaluppi, S., and Krings, T.** 2009. Dynamic CT angiography and CT perfusion employing a 320-detector row CT. Clinical Neuroradilogy; **23:**187-196.
12. **Cohenpour, M., Strauss, S., Gottlieb, P., Peer, A., Rimon, U., Stav, K., and Gayer, G.** 2007. Pseudoaneurysm of the renal artery following partial nephrectomy: imaging findings and coil embolization. Clin Radiol; **62:**1104-9.
13. **Fürst, H., Hartl, W.H., Löhe, F., and Schildberg, F.W.** 2000. Colon interposition for esophageal replacement: an alternative technique based on the use of the right colon. Ann Surg; **231:**173-8.
14. **Kakizawa, H., Toyota, N., Hieda, M., Ishida, M., Takeda, T., Matsuura, K., Hirai, N., Tachikake, T., Matsuura, N., Kohno, S., Yananoue, T., and Ito, K.** 2007. Traumatic mesenteric bleeding managed solely with transcatheter embolization. Radiat Med; **25:**295-8.
15. **Görich, J., Rilinger, N., Sokiranski, R., Krämer, S., Schütz A., Sunder-Plassmann, L., and Pamler, R.** 2000. Embolization of type II endoleaks fed by the inferior mesenteric artery: using the superior mesenteric artery approach. J Endovasc Ther; **7:**297-301.
16. **Svanholm, H., Starklint, H., Gundersen, H.J., Fabricius, J., Barlebo, H., and Olsen, S.** 1989. Reproducibility of histomorphologic diagnoses with special reference to the kappa statistic. APMIS; **97**:689-98.
17. **Leng, S., Zhuang, T., Nett, B.E., and Chen, G.H.** 2005. Exact fan-beam image reconstruction algorithm for truncated projection data acquired from an asymmetric half-size detector. Phys Med Bio; **50:**1805-1820.
18. **Annop, K.P., and Rajgopal, K.** 2007. Estimation of missing data using windowed linear prediction in laterally truncated projections in cone-beam CT. Conf Proc IEEE Eng Med Bio Soc; **2007:**2903-2906.
19. **Endo, M., Mori, S., Tsunoo, T., and Miyazaki, H.** 2006. Magnitude and effects of x-ray scatter in a 256-slice CT scanner. Med Phys; **33:**3359-3368.
20. **Sun, Y., Hou, Y., and Hu, J.** 2007. Reduction of artifacts induced by misaligned geometry in cone-beam CT. IEEE Trans Biomed Eng; **54:**1461-1471.
21. **Kobayashi, T., Hayashi, T., Funabasama, S., Tsukagoshi, S., Minami, M., and Moriyama N.** 2008. Three-dimensional perfusion imaging of hepatocellular carcinoma using 256-slice multidetector-row computed tomography. Radiat Med; **26:**557-561.